Organic Geochemistry 39 (2008) 646–657

Contents lists available at ScienceDirect

Organic Geochemistry

journal homepage: www.elsevier.com/locate/orggeochem

# Distribution and isomerization of $C_{31}$–$C_{35}$ homohopanes and $C_{29}$ steranes in oligocene saline lacustrine sediments from Qaidam Basin, Northwest China

Changchun Pan [a,*], Dehua Peng [a,b], Min Zhang [a,b], Linping Yu [a], Guoying Sheng [a], Jiamo Fu [a]

[a] State Key Laboratory of Organic Geochemistry, Guangzhou Institute of Geochemistry, Chinese Academy of Sciences, Guangzhou 510640, China
[b] Research Institute of Petroleum Exploration and Development, Qinghai Oil Company, CNPC, China

ARTICLE INFO

*Article history:*
Received 13 January 2008
Received in revised form 29 February 2008
Accepted 29 February 2008
Available online 10 March 2008

ABSTRACT

The 22S/(22S + 22R) ratios for $C_{31}$–$C_{35}$ homohopanes and the 20S/(20S + 20R) ratio for $C_{29}$ steranes were measured by gas chromatography–mass spectrometry (GC–MS) on six Oligocene saline lacustrine rock samples from a borehole located in the western Qaidam Basin, northwest China. These ratios vary significantly and irregularly with burial depth from 2831 m to 3054 m around the threshold of the oil generation window. In addition, 22S/(22S + 22R) ratios also vary substantially among different homologs within the same sample, generally decreasing from $C_{31}$ to $C_{35}$ homohopanes. The distribution patterns of homohopanes for the six samples are unusual, such as, $C_{31} < C_{32} > C_{33} > C_{34} < C_{35}$, or $C_{31} > C_{32} > C_{33} < C_{34} < C_{35}$, or $C_{31} < C_{32} > C_{33} < C_{34} < C_{35}$. All of these observations can be mainly ascribed to the release of bound hopanes and steranes from kerogen and other macromolecules.

The 22S/(22S + 22R) ratios of $C_{31}$, $C_{32}$ and $C_{33}$ homohopanes decreased, while that of $C_{34}$ homohopanes increased for two samples, YHS1 and YHS6, after pyrolysis at low temperatures (180–270 °C). A major reversal of 20S/(20S + 20R) ratio for $C_{29}$ steranes was observed at 240 °C for sample YHS1, but at 270 °C for sample YHS6. The distributions of homohopanes for these two samples after pyrolysis changed from their original patterns toward the normal pattern $C_{31} > C_{32} > C_{33} > C_{34} > C_{35}$. These results reflect the influences of thermal degradation and direct isomerization of the free biomarkers and the release of bound biomarkers from kerogen and other macromolecules during pyrolysis.



## 1. Introduction

Isomerization ratios of 22S/(22S + 22R) for homohopanes and 20S/(20S + 20R) for $C_{29}$ steranes are among the most frequently used biomarker thermal maturity parameters (e.g., Ensminger et al., 1974, 1977; Mackenzie et al., 1980; Seifert and Moldowan, 1980, 1986; Peters and Moldowan, 1993). The 22S/(22S + 22R) ratio is usually measured on the $C_{31}$ or $C_{32}$ homohopanes and rises from 0 to about 0.6 during maturation (Peters et al., 2005). The proposed thermodynamic equilibrium mixture is in the range of 0.57–0.62 (Seifert and Moldowan, 1980; van Duin et al., 1997). This equilibrium value is attained at a relatively early stage of oil generation in petroleum source rocks. The 20S/(20S + 20R) ratio of $C_{29}$ steranes rises from 0 to about 0.50 (Mackenzie et al., 1980; Mackenzie, 1984; Seifert and Moldowan, 1986).

Previous pyrolysis studies have documented the reversal of isomerization ratios of hopanes and steranes with increased temperature or heating time (e.g., Lewan et al., 1986; Lu et al., 1989; Peters et al., 1990). This reversal phenomenon was also observed for biomarker maturation in sediments heated by an igneous intrusion (Bishop and

* Corresponding author. Tel.: +86 20 85290183; fax: +86 20 85290706.
*E-mail address:* cpan@gig.ac.cn (C. Pan).

0146-6380/$ - see front matter © 2008 Elsevier Ltd. All rights reserved.
doi:10.1016/j.orggeochem.2008.02.024

Abbott, 1993; Farrimond et al., 1996). In these previous studies, it was proposed that the release of the kerogen bound biomarkers could be the primary factor for the observed reversal (e.g., Lu et al., 1989; Peters et al., 1990; Farrimond et al., 1996). Numerous recent studies have demonstrated clearly that the hopanes and steranes released from kerogen by catalytic hydropyrolysis have low maturities compared with their free counterparts in bitumen (Love et al., 1995, 1996, 1997, 1998; Bishop et al., 1998; Murray et al., 1998). The reversal of isomerization ratios of homohopanes and steranes was also reported in natural sediments with burial. For example, Curiale and Odermatt (1989) observed a trend away from equilibrium with increasing depth in Monterey Formation rocks from the Santa Maria Basin, USA. Strachan et al. (1989) observed a reversal in the $C_{29}$ sterane 20S/(20S + 20R) ratio with depth in the Cape Range No. 2 well, Australia, and ascribed it to the effect of sediment matrix variation.

There are three end member processes that may control the isomerization ratios of homohopanes and steranes: (1) direct isomerization of isomer A to isomer B, (2) differences in the relative rates of generation of these two isomers from kerogen or another non-hydrocarbon fraction, and (3) differences in the relative rates of cracking of these two isomers to one or more products other than the isomers (Farrimond et al., 1998). The 22S/(22S + 22R) ratios measured among $C_{31}$–$C_{35}$ homohopanes are usually similar, within a variation range less than 0.05. This result implies that the rates of these three processes among $C_{31}$–$C_{35}$ homohopanes are similar for a given sample.

The 22S/(22S + 22R) ratios for the $C_{31}$–$C_{35}$ 17α-homohopanes may differ slightly, or even significantly in some cases. Zumberge (1987) determined average 22S/(22S + 22R) ratios for the $C_{31}$–$C_{35}$ homohopanes of 27 heavy crude oils. The averaged values at $C_{31}$, $C_{32}$, $C_{33}$, $C_{34}$, and $C_{35}$ for 22S/(22S + 22R) ratios are 0.55, 0.58, 0.60, 0.62, and 0.59, respectively. The author suggested that the equilibrium ratios increase with carbon number for $C_{31}$–$C_{34}$ homologs (Zumberge, 1987). Köster et al. (1997) found that the 22S/(22S + 22R) ratios vary substantially from $C_{31}$ to $C_{35}$ homohopanes in some immature organic sulfur rich samples from carbonate/marlstone sequences. These ratios regularly increase from $C_{31}$ to $C_{35}$ homologs, e.g., values as low as 0.18 for the $C_{31}$ homologs to 0.54 for the $C_{35}$ homologs in one of their samples. This result is explained by steric hindrance of the isomerization at C-22 of condensed type hopanoid sulphides and sulphoxides having 22R stereochemistry. Upon maturation these skeletons are released as hydrocarbons, which can lead to low 22S/(22S + 22R) ratios (Köster et al., 1997).

Homohopanes ($C_{31}$–$C_{35}$) are generally believed to originate from bacteriohopanepolyols, which are synthesized as membrane lipids by bacteria of diverse taxonomic groups (Ourisson et al., 1979, 1984; Farrimond et al., 2003). The relative distribution of homohopanes has been used as an indicator of the redox potential (Eh) during deposition of source rocks (Peters and Moldowan, 1991; Moldowan et al., 1992). The "$C_{35}$-homohopane index" is the ratio of $C_{35}$/($C_{31}$–$C_{35}$). High $C_{35}$-homohopane indices are typical of marine, low Eh environments of deposition (Peters and Moldowan, 1991). Sinninghe Damsté et al. (1995) have shown that selective preservation of the $C_{35}$ skeleton by sulfur incorporation is the most likely mechanism for the relative enrichment of $C_{35}$ homohopanes under anoxic conditions. However, homohopane distributions can be altered by secondary processes. Peters and Moldowan (1991) demonstrated that: (1) the $C_{35}$-homohopane index decreases with increasing API gravity and thermal maturity of related oils from the Monterey Formation, offshore California; and (2) biodegradation can result in selective loss of high or low molecular weight homologs, depending on the microbial population in the reservoir.

In the present study, we document the 22S/(22S + 22R) ratios of homohopanes, 20S/(20S + 20R) ratios of $C_{29}$ regular steranes, and the distributions of $C_{31}$–$C_{35}$ homohopanes for six rocks within a 220 m interval of Oligocene strata (lower Ganchaigou Formation, E3) from YH-103 well in the western Qaidam Basin. The ratios of 22S/(22S + 22R) homohopanes and 20S/(20S + 20R) $C_{29}$ regular steranes vary significantly and irregularly with burial depth for these six samples. The 22S/(22S + 22R) ratios also vary substantially from $C_{31}$ to $C_{35}$ homohopanes within the same sample with a variation trend opposite to those reported previously by Zumberge (1987) and Köster et al. (1997). In order to investigate the variations of the distribution and isomerization of homohopanes and steranes with increasing temperature and thermal maturity, pyrolysis experiments on two of these six rock samples were performed in a confined system (Au capsules). We hope that our results can extend understanding of the mechanisms that control biomarker maturity parameters. In addition, oil samples from the major oil fields in this region, including the largest one, the Yuejin oil field, were believed to be low maturity based on biomarker maturity parameters (Huang et al., 1989, 1991, 1994, 1999; Hanson et al., 2001; Peng, 2005; Zhu et al., 2005). Our results may also improve understanding of the origin of these low maturity oils.

## 2. Samples and experimental

### 2.1. Samples

Six samples of calcareous mudstones and limestones were collected from Oligocene strata (lower Ganchaigou Formation, E3; burial depths of 2831–3054 m) from the YH-103 well in the western Qaidam Basin, northwest China. The lower Ganchaigou Formation contains the principal source rocks for the oil fields found in this region and was deposited in a saline lacustrine environment (e.g., Hanson et al., 2001; Zhu et al., 2005). Among these six samples, YHS1 to YHS6, the shallowest sample YHS1 with relatively high total organic carbon content (TOC) and low content of carbonate minerals, and the deepest sample YHS6 with the lowest TOC and highest content of carbonate minerals were selected for pyrolysis experiments (Table 1). These two samples lack vitrinite. To evaluate the maturities of these samples after pyrolysis at various temperatures, a coal sample having a vitrinite reflectance (Ro) of 0.42% from the Jurassic coal measures of Tuha basin, northwest China, was selected for the pyrolysis experiments.

**Table 1**
The gross geochemical parameters of rock samples

| | Depth (m) | Carbonate (%) | TOC (%) | S1 (mg/g) | S2 (mg/g) | HI | $T_{max}$ (°C) | PI | Bit | Sat (%) | Aro (%) | Res (%) | Asp (%) |
|---|---|---|---|---|---|---|---|---|---|---|---|---|---|
| YHS1 | 2831.6 | 25.56 | 1.03 | 0.61 | 5.19 | 504 | 423 | 0.11 | 244 | 49.3 | 12.8 | 24.7 | 13.2 |
| YHS2 | 2845.1 | 43.73 | 1.12 | 0.46 | 6.67 | 596 | 419 | 0.06 | 302 | 29.0 | 20.3 | 36.2 | 14.5 |
| YHS3 | 3018.1 | 26.71 | 0.84 | 0.41 | 2.82 | 336 | 427 | 0.13 | 250 | 58.6 | 10.4 | 23.2 | 7.7 |
| YHS4 | 3022.1 | 24.83 | 0.86 | 0.30 | 2.94 | 342 | 427 | 0.09 | 308 | 53.6 | 12.7 | 27.0 | 6.7 |
| YHS5 | 3043.8 | 37.02 | 0.78 | 0.29 | 4.04 | 518 | 430 | 0.07 | 254 | 34.2 | 17.1 | 38.7 | 10.1 |
| YHS6 | 3053.9 | 55.57 | 0.48 | 0.09 | 1.42 | 296 | 431 | 0.06 | 210 | 41.3 | 11.5 | 33.7 | 13.5 |

HI: hydrogen index (mg HC/g TOC) = 100×S2/TOC; PI = S1/(S1 + S2); bit: bitumen (mg/g TOC); sat: saturates; aro: aromatics; res: resins; asp: asphaltenes.

### 2.2. Analyses of the content of carbonate minerals and total organic carbon content (TOC)

The six samples were first ground into powder (about 200 mesh). About 2 g of powder from each sample was treated with 6N HCl at 80 °C for 8 h and then washed with distilled water to pH 6. The amount of carbonate minerals was obtained by the gravimetric method. After HCl treatment, the total organic carbon content (TOC) of the remaining sample was measured using an Elementar vario EL III, an advanced model of elemental analyzer (C, H, N and O) for kerogen. TOC of the original sample was calculated based on the measured TOC and the amount of carbonate minerals.

### 2.3. Bitumen extraction and fractionation

The powdered samples (about 80 g each) were Soxhlet extracted with azeotropic dichloromethane:methanol (93:7, v/v) for 72 h to obtain bitumen. The solvent free bitumen was diluted with about 1 ml dichloromethane, and then deasphaltened using about 50 ml hexane. These samples were fractionated on a silica-alumina column using hexane, benzene and methanol as eluants to yield saturated, aromatic, and resin fractions, respectively. The saturated fractions were further analyzed by GC-FID and GC–MS.

### 2.4. GC and GC–MS analyses

Gas chromatographic (GC) analysis of the saturated fractions was performed on an HP6890 GC fitted with a 30 m × 0.32 mm i.d. HP-5 column with a film thickness of 0.25 μm and using nitrogen carrier gas. The GC oven temperature was held initially at 70 °C for 5 min, ramped from 80 to 290 °C at 4 °C/min, and then held at 290 °C for 30 min. Gas chromatographic–mass spectrometric (GC–MS) analysis of the saturated fractions was carried out using a Micromass Platform II interfaced to an HP5890 GC fitted with a 30 m × 0.25 mm i.d. HP-5 ms column with a film thickness of 0.25 μm and using helium carrier gas. The GC oven temperature was initially held at 80 °C for 5 min, ramped from 80 to 120 °C at 8 °C/min, from 120 to 290 °C at 2 °C/min, and then held at 290 °C for 30 min.

### 2.5. Pyrolysis in a confined system

The approach of pyrolysis in a confined system was first applied on hydrocarbon source rocks by Monthioux et al. (1985, 1986). In the present studies, pyrolysis experiments on two rock samples (YHS1 and YHS6) and a coal were performed in a confined system (Au capsules) at a fixed pressure of 50 MPa and temperatures of 180, 210, 240, 270, 300, and 320 °C. For each run, about 5 g of powdered sample YHS1 (unextracted) mixed with 3 wt% water was placed into two Au capsules (6 mm outside diameter, 0.25 mm wall thickness, and 80 mm length) while about 7.5 g powdered sample YHS6 (unextracted) with 3 wt% water was placed into three Au capsules. In addition, about 100 mg powdered coal sample with 3% water was placed into a Au capsule. The pyrolysis results among the duplicate Au capsules have excellent repeatability (e.g., Pan et al., 2006). The 3% water was added with the consideration that these rocks have porosity of about 6%. The capsules were welded at one end before loading samples. Once loaded, the open end of each capsule was purged with argon before being squeezed in a vise to create an initial seal, which was subsequently welded in the presence of argon. During welding, the previously welded end was submerged in cold water to prevent heating of reactants.

Each loaded capsule containing the rock or coal sample was placed into a pressure vessel. Our experimental system permits 14 pressure vessels to be placed in a single large furnace. A fan at the bottom of the furnace maintained uniform temperature in the vessels during the experiment. The vessels were previously filled with water. The internal pressure of the vessels, which were connected to each other with tubing, was adjusted to 50 MPa by pumping water into the vessels before heating. Pressure was maintained automatically by pumping water into or out of the vessels during the pyrolysis experiments. The vessels were heated to the desired temperature during 2 h, and then, heated isothermally for 72 h. A thermocouple is placed in the furnace attached to one of these vessels. After heating, the vessels were quenched to room temperature in cold water within 10 min. During quenching, the pressure was held at 50 MPa to prevent the capsules from leaking. After cooling, the pressure inside the vessel was gradually reduced to atmosphere pressure.

After heating, the samples were Soxhlet extracted and fractionated. The saturated fractions obtained were analyzed by GC and GC–MS. These methods were the same as for the six rocks described above.

## 3. Results and discussion

### 3.1. Gross geochemical properties

The gross geochemical data for the six samples are shown in Table 1. The amounts of carbonate minerals in the six samples range from 24.83% to 55.57%. The total organic carbon contents (TOC) range from 0.48% to 1.12%. Rock-Eval

pyrolysis hydrogen index (HI) values range from 293 to 595 mg/g TOC (Table 1). Rock-Eval pyrolysis Tmax ranges from 419 to 430 °C. The amount of extracted bitumen ranges from 210 to 308 mg/g TOC. The amount of saturated fraction of the extracted bitumen ranges from 29.0% to 58.6%. Vitrinite reflectance values for these rock samples were not obtained because they lack vitrinite. The amounts of bitumen and saturated fractions suggest that these rock samples are near or have reached the oil generation threshold.

### 3.2. Molecular compositions

#### 3.2.1. n-Alkanes and acyclic isoprenoids

The gas chromatograms of the saturate fractions of extracts from the six rock samples are shown in Fig. 1 and the related parameters are listed in Table 2. All six samples show a strong even over odd predominance of normal alkanes with OEP values ranging from 0.65 to 0.86. They also contain a relatively high abundance of phytane, with ratios of Pr/$n$-$C_{17}$, Ph/$n$-$C_{18}$, and Pr/Ph ranging from 0.45 to 1.05, 1.40 to 3.78 and 0.18 to 0.36, respectively.

#### 3.2.2. Hopanes and steranes

*M/z* 191 and *m/z* 217 mass chromatograms of the six samples are shown in Fig. 2, and hopane and sterane parameters are listed in Table 2. All six samples contain very little Ts, but abundant gammacerane with the gammacerane/$C_{30}$ hopane ratio ranging from 0.64 to 1.24.

All samples contain very low amounts of diasteranes compared with regular steranes. Samples YHS1 and YHS2 contain low amounts of $C_{28}$ and $C_{29}$ steranes relative to $C_{27}$ steranes compared with the other samples.

The 22S/(22S + 22R) ratios for $C_{31}$–$C_{35}$ homohopanes generally decrease in the order $C_{31} > C_{32} > C_{33} > C_{34} > C_{35}$ for all the six samples, except for sample YHS2 ($C_{31} > C_{32} < C_{33} > C_{34} < C_{35}$, Fig. 3a, Table 2). Although the ratios of all $C_{31}$–$C_{35}$ homohopanes vary significantly and irregularly among the six samples with burial depth, their variation trends are consistent with each other, except for the $C_{33}$ and $C_{35}$ homohopanes in sample YHS2 (Fig. 3a).

The proportions of $C_{31}$–$C_{35}$ homohopanes change substantially and irregularly among the six samples with burial depth. The distribution patterns of $C_{31}$–$C_{35}$ homohopanes are $C_{31} < C_{32} > C_{33} > C_{34} < C_{35}$ for samples YHS1, YHS2 and YHS6, $C_{31} > C_{32} > C_{33} < C_{34} < C_{35}$ for sample YHS3, and $C_{31} < C_{32} > C_{33} < C_{34} < C_{35}$ for samples YHS4 and YHS5 (Table 2, Figs. 2 and 3b). All of these patterns are unusual to source rock and oil samples (e.g., Peters et al., 2005).

The $C_{29}$ sterane 20S/(20S + 20R) ratio for the six samples ranges from 0.111 to 0.250. It varies irregularly with burial depth, but the variation trend is roughly consistent with that of the 22S/(22S + 22R) ratios for homohopanes, especially $C_{31}$, $C_{32}$ and $C_{34}$ homohopanes (Table 2, Fig. 3a).

### 3.3. Variations of hopanes and steranes during pyrolysis experiments

#### 3.3.1. Variation of vitrinite reflectance Ro% of the coal sample during pyrolysis

As listed in Table 3, the vitrinite reflectance value of the coal sample increases slowly during pyrolysis at low tem-

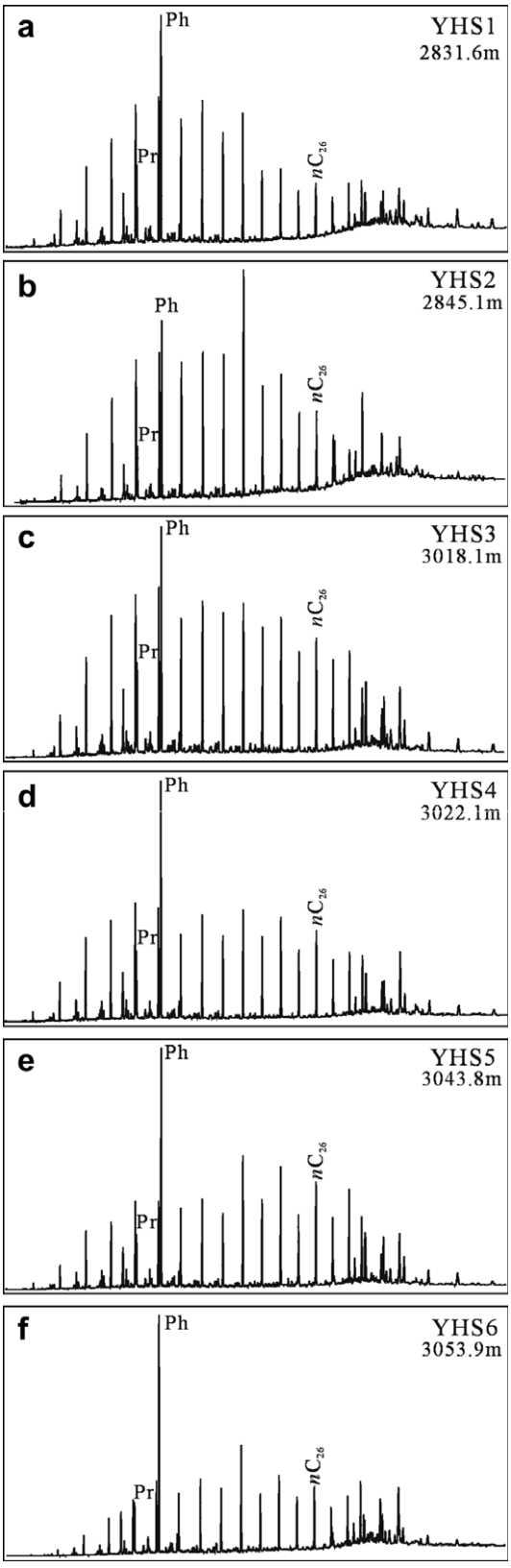


**Fig. 1.** Gas chromatograms of the saturated fractions of samples YHS1–YHS6.

**Table 2**
Molecular parameters of the initial bitumen of the six rock samples

| | OEP | Pr/$n$-$C_{17}$ | Ph/$n$-$C_{18}$ | Pr/Ph | 1 | 2 | 3 | 4 | 5 | 6 | 7 | 8 | 9 | 10 | 11 | 12 |
|---|---|---|---|---|---|---|---|---|---|---|---|---|---|---|---|---|
| YHS1 | 0.75 | 0.61 | 1.85 | 0.32 | 0.86 | 0.563 | 0.512 | 0.489 | 0.442 | 0.430 | 0.250 | 0.282 | 0.315 | 0.130 | 0.119 | 0.154 |
| YHS2 | 0.63 | 0.45 | 1.40 | 0.31 | 1.21 | 0.532 | 0.476 | 0.500 | 0.405 | 0.422 | 0.168 | 0.220 | 0.372 | 0.119 | 0.101 | 0.188 |
| YHS3 | 0.86 | 0.61 | 1.59 | 0.36 | 0.94 | 0.576 | 0.507 | 0.453 | 0.413 | 0.344 | 0.168 | 0.259 | 0.245 | 0.127 | 0.153 | 0.216 |
| YHS4 | 0.78 | 0.65 | 2.56 | 0.26 | 0.64 | 0.511 | 0.424 | 0.374 | 0.330 | 0.293 | 0.111 | 0.190 | 0.228 | 0.097 | 0.214 | 0.271 |
| YHS5 | 0.66 | 0.64 | 3.44 | 0.18 | 1.24 | 0.515 | 0.433 | 0.411 | 0.359 | 0.357 | 0.160 | 0.155 | 0.228 | 0.108 | 0.160 | 0.351 |
| YHS6 | 0.65 | 1.05 | 3.78 | 0.21 | 0.73 | 0.512 | 0.417 | 0.417 | 0.341 | 0.336 | 0.180 | 0.198 | 0.280 | 0.097 | 0.096 | 0.328 |

OEP: odd-even predominance for $n$-alkanes in the range from $C_{21}$ to $C_{25}$; 1: gammacerane/hopane; 2–6: 22S/(22S + 22R) ratios for $C_{31}$, $C_{32}$, $C_{33}$, $C_{34}$, and $C_{35}$ homohopanes, respectively; 7: 20S/(20S + 20R) $C_{29}$ steranes; 8: $C_{31}/(C_{31}–C_{35})$ homohopanes; 9: $C_{32}/(C_{31}–C_{35})$ homohopanes; 10: $C_{33}/(C_{31}–C_{35})$ homohopanes; 11: $C_{34}/(C_{31}–C_{35})$ homohopanes; 12: $C_{35}/(C_{31}–C_{35})$ homohopanes.

peratures, from the initial value 0.42 to 0.53 at 270 °C. It increases rapidly to 0.74 at 300 °C and 0.86 at 320 °C.

### 3.3.2. Sample YHS1

As demonstrated in Table 3 and Fig. 4a, the 22S/(22S + 22R) ratio for $C_{31}$ homohopanes decreased from the initial value of 0.563–0.512 at 180 °C. It varied slightly between 0.498 and 0.512 at temperatures 210–300 °C, and finally increased to 0.535 at 320 °C. The ratios for $C_{32}$ and $C_{33}$ homohopanes varied similarly to that for $C_{31}$ homohopanes with temperature. However, the ratio for $C_{34}$ homohopanes increased significantly at 180 °C, contrary to that for $C_{31}$–$C_{33}$ homohopanes. The ratio for $C_{35}$ homohopanes also increased at 180 °C, but had a major reversal at 270 °C. The 20S/(20S + 20R) ratio for $C_{29}$ steranes decreased from 180 to 240 °C, and then increased rapidly at higher temperatures.

The proportions of $C_{31}$–$C_{35}$ homohopanes are listed in Table 3 and shown in Fig. 4b. The proportions of homohopanes varied substantially during pyrolysis. The distribution of $C_{31}$–$C_{35}$ homohopanes changed from the initial pattern $C_{31} < C_{32} > C_{33} > C_{34} < C_{35}$ into $C_{31} > C_{32} > C_{33} > C_{34} > C_{35}$ at 180 °C, which is observed frequently in source rocks and oils (e.g., Peters et al., 2005). At 210–320 °C, the proportions of $C_{31}$–$C_{35}$ homohopanes varied slightly, but the distribution pattern remained unchanged.

### 3.3.3. Sample YHS6

The variation trends for 22S/(22S + 22R) ratios of $C_{31}$–$C_{35}$ homohopanes, 20S/(20S + 20R) ratio of $C_{29}$ steranes, and proportions of $C_{31}$–$C_{35}$ homohopanes for sample YHS6 are generally similar to those of sample YHS1 (Table 3 and Fig. 4c and d). However, some minor differences can be observed in hopane and sterane maturation behavior between YHS1 and YHS6 during pyrolysis. The 22S/(22S + 22R) ratios for $C_{31}$ and $C_{33}$ homohopanes in YHS6 decreased to a greater extent than in YHS1 after pyrolysis at 180 °C (Fig. 4a and c). The 20S/(20S + 20R) ratio for $C_{29}$ steranes in YHS6 was lowest at 270 °C, rather than 240 °C as observed for YHS1 (Fig. 4b and d).

The distribution of $C_{31}$–$C_{35}$ homohopanes changed from the original pattern $C_{31} < C_{32} > C_{33} > C_{34} < C_{35}$ towards the normal pattern $C_{31} > C_{32} > C_{33} > C_{34} > C_{35}$ with temperature increasing during pyrolysis. During this process, the ratios of $C_{31}/\Sigma(C_{31}–C_{35})$ and $C_{32}/\Sigma(C_{31}–C_{35})$ homohopanes increased while the ratio of $C_{35}/\Sigma(C_{31}–C_{35})$ homohopanes decreased. Because the distribution of homohopanes remains $C_{31} > C_{32} > C_{33} > C_{34} < C_{35}$ at 320 °C, the transformation to the normal pattern is not yet completed (Table 3, Fig. 4d). According to our analytical data for 38 oil samples collected from western Qaidam Basin, 26 relatively high maturity samples have the normal distribution pattern, 11 moderate maturity samples have the pattern $C_{31} > C_{32} > C_{33} > C_{34} < C_{35}$, and one low maturity sample has the pattern $C_{31} < C_{32} > C_{33} > C_{34} < C_{35}$.

## 3.4. Mechanisms controlling homohopane and sterane distributions and isomerization ratios

Variations in the 22S/(22S + 22R) ratio for $C_{31}$–$C_{35}$ homohopanes and the 20S/(20S + 20R) ratio for $C_{29}$ steranes are related to the isomerization rate between the free R and S isomers, the decomposition rates of both free isomers, and the release rates of both bound isomers from kerogen and other macromolecules (Lu et al., 1989; Peters et al., 1990; Farrimond et al., 1998). Both the isomerization and decomposition of free homohopanes and steranes in bitumen or oil lead to the increase in isomerization ratios. Several studies have demonstrated that increasing isomerization ratios of hopanes and steranes are due mainly to the decomposition (thermal degradation) rather than the direct isomerization (Larcher et al., 1988; Requejo, 1994; Dzou et al., 1995; Farrimond et al., 1998). In contrast, release of bound homohopanes and steranes from kerogen and other macromolecules leads to decreasing isomerization ratios (e.g. Lu et al., 1989; Peters et al., 1990; Bishop et al., 1998).

For both samples YHS1 and YHS6, variations in the proportions of $C_{31}$–$C_{35}$ homohopanes during pyrolysis can be interpreted to result from increasing decomposition rate of the free homohopanes with greater carbon number, or decreasing release rate of bound homohopanes from kerogen and the other macromolecules (resin and asphaltene) with greater carbon number, or both (Table 3, Fig. 4b and d). For YHS1, the variations in 22S/(22S + 22R) ratios between the original bitumen and the pyrolysate at 180 °C for $C_{31}$, $C_{32}$, $C_{33}$, $C_{34}$ and $C_{35}$ homohopanes are −0.045, −0.017, −0.014, 0.060, and 0.007, respectively, and the variations in the ratios of $C_{31}/\Sigma(C_{31}–C_{35})$, $C_{32}/\Sigma(C_{31}–C_{35})$, $C_{33}/\Sigma(C_{31}–C_{35})$, $C_{34}/\Sigma(C_{31}–C_{35})$ and $C_{35}/\Sigma(C_{31}–C_{35})$ are 0.087, 0.050, −0.025, −0.035, and −0.076, respectively. It appears that the release of bound homohopanes containing R isomers from kerogen and the other macromolecules could be the dominant factor influencing 22S/(22S + 22R)

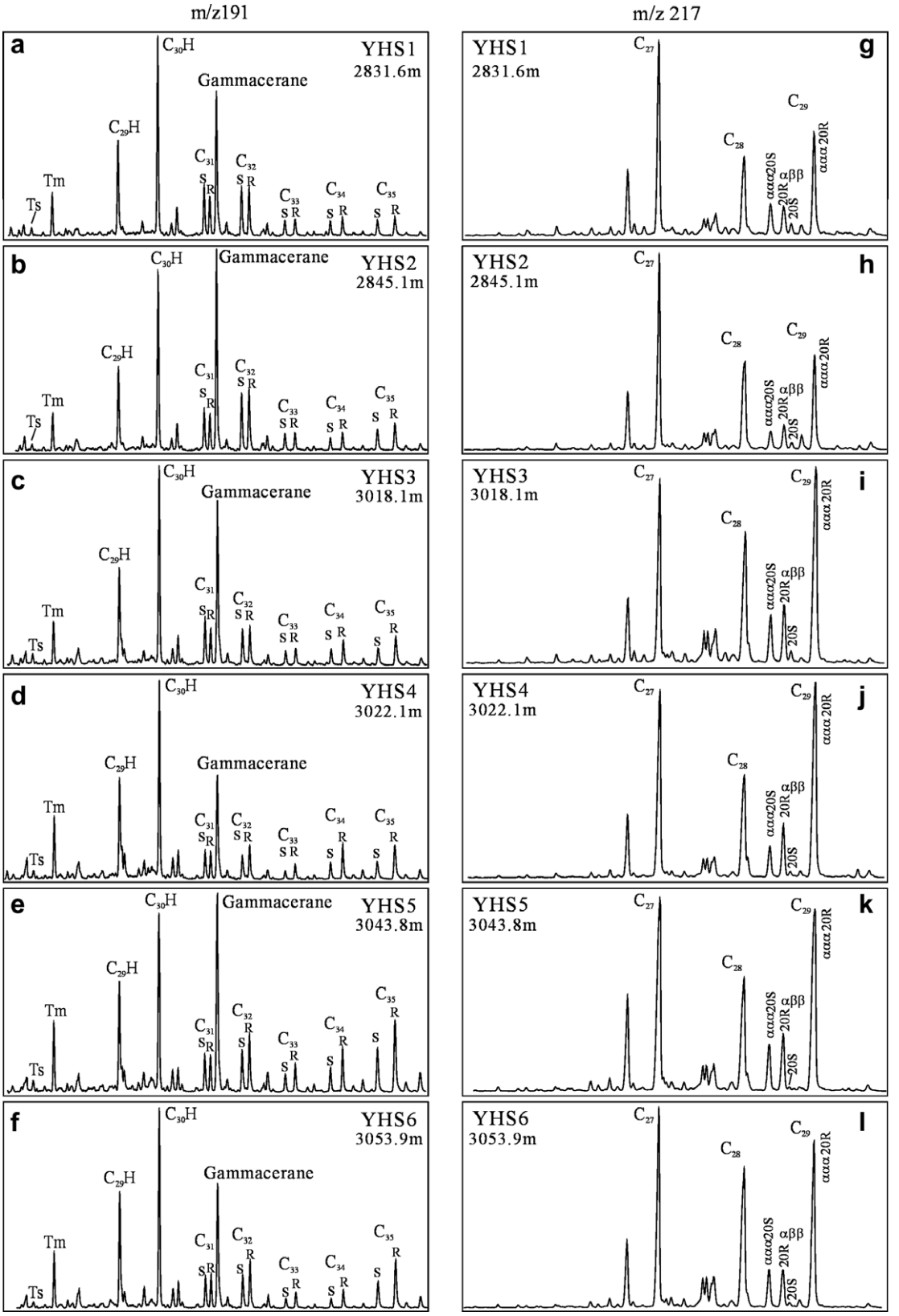


**Fig. 2.** Hopane and sterane mass chromatograms of samples YHS1–YHS6. (a–f) Hopane mass chromatograms (*m/z* 191); (g–l) sterane mass chromatograms (*m/z* 217).

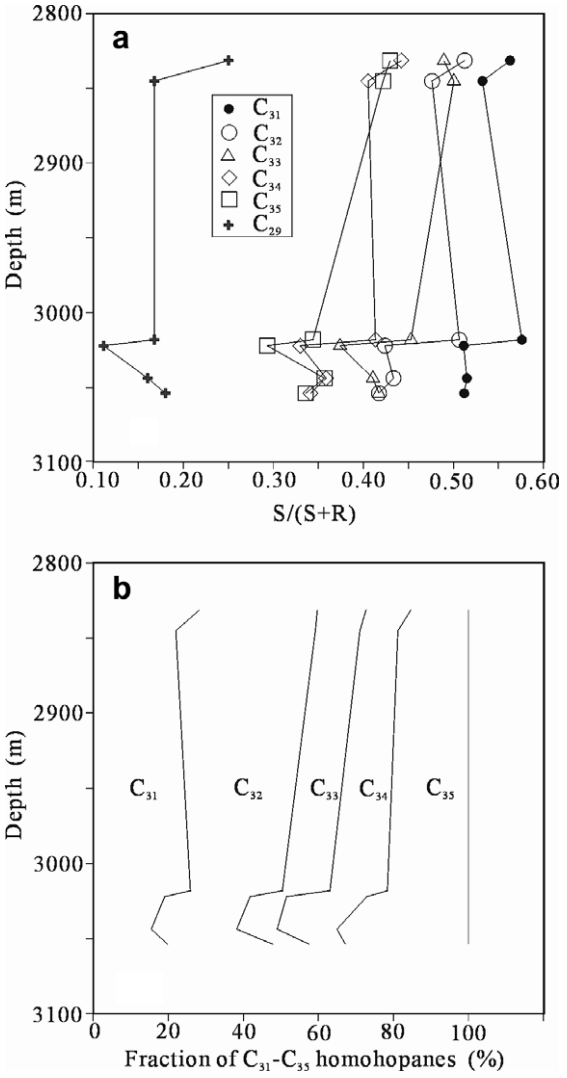


**Fig. 3.** Isomerization ratios and distribution of homohopanes and steranes of samples YHS1–YHS6. (a) 20S/(20S + 20R) ratio of $C_{29}$ steranes and 22S/(22S + 22R) ratios of $C_{31}$–$C_{35}$ homohopanes; (b) distribution of $C_{31}$–$C_{35}$ homohopanes.

ratios of $C_{31}$–$C_{33}$ homohopanes at this temperature. However, the increase of 22S/(22S + 22R) ratios of $C_{34}$ and $C_{35}$ homohopanes demonstrates that decomposition and direct isomerization were important for $C_{34}$ and $C_{35}$ homohopanes at this temperature.

The greater decrease of $C_{35}/\Sigma(C_{31}–C_{35})$ ratio than $C_{34}/\Sigma(C_{31}–C_{35})$ ratio implies that $C_{35}$ homohopanes were decomposed to a greater extent than $C_{34}$ homohopanes. However, the smaller increase in the 22S/(22S + 22R) ratio for $C_{35}$ homohopanes than the $C_{34}$ homohopanes indicates that larger amounts of bound $C_{35}$ homohopanes were released from kerogen and other macromolecules than those of bound $C_{34}$ homohopanes.

A major reversal can be observed for 22S/(22S + 22R) ratios of $C_{33}$ and $C_{35}$ homohopanes at 270 °C (Table 3, Fig. 4a). This result suggests that peak generation of $C_{33}$ and $C_{35}$ homohopanes from the cracking of kerogen and other macromolecules occurred at this temperature. At higher temperatures (300–320 °C), we speculate that the release of $C_{33}$ and $C_{35}$ homohopanes was outpaced by decomposition and direct isomerization rates became higher than those at 270 °C. As a result, the 22S/(22S + 22R) ratios for $C_{33}$ and $C_{35}$ homohopanes increased at 300 and 320 °C. A similar reversal occurred for the 20S/(20S + 20R) ratio of $C_{29}$ steranes at 240 °C, and can be interpreted in the same manner.

For YHS6, the variations in the 22S/(22S + 22R) ratios for $C_{31}$, $C_{32}$, $C_{33}$, $C_{34}$ and $C_{35}$ homohopanes are −0.072, −0.010, −0.054, 0.058, and 0.006, respectively, and the variations in the ratios of $C_{31}/\Sigma(C_{31}–C_{35})$, $C_{32}/\Sigma(C_{31}–C_{35})$, $C_{33}/\Sigma(C_{31}–C_{35})$, $C_{34}/\Sigma(C_{31}–C_{35})$ and $C_{35}/\Sigma(C_{31}–C_{35})$ are 0.084, 0.057, 0.000, −0.017, and −0.122, respectively during pyrolysis at 180 °C. The major decrease of 22S/(22S + 22R) ratios for $C_{31}$ and $C_{33}$ homohopanes demonstrates that the release of bound homohopanes strongly affected these ratios. In contrast, the major increase of 22S/(22S + 22R) ratio for $C_{34}$ homohopanes suggests that decomposition and isomerization played dominant roles in controlling this ratio. The 22S/(22S + 22R) ratios for $C_{32}$ and $C_{35}$ homohopanes indicate that the effects of the decomposition and isomerization of free homohopanes and the release of bound homohopanes appear roughly balanced. A small reversal of 22S/(22S + 22R) ratio for $C_{35}$ homohopanes at 240 °C suggests a minor peak generation stage of these homohopanes from the cracking of kerogen and other macromolecules (Fig. 4c). The substantial increase of 22S/(22S + 22R) ratios for all $C_{31}$–$C_{35}$ homohopanes from 300 to 320 °C can be interpreted to indicate that all bound homohopanes were released within the first few hours of heating, and then, decomposition and isomerization prevailed within the remaining heating time at 320 °C.

A reversal of 20S/(20S + 20R) $C_{29}$ steranes for YHS6 occurred at 270 °C, rather than 240 °C as for YHS1 (Fig. 4a and c). This suggests that there could be different release kinetics for these compounds from kerogen and macromolecules between these two samples.

The distribution of $C_{27}$, $C_{28}$ and $C_{29}$ regular steranes for sample YHS6 varied significantly during pyrolysis: the relative abundances of $C_{28}$ and $C_{29}$ regular steranes increased at low temperatures (180–240 °C), and decreased at high temperatures (270–320 °C) (Fig. 5). Although the absolute amounts of steranes were not quantified in our study the substantial variation in the distribution of $C_{27}$–$C_{29}$ steranes can be mainly ascribed to the release of the bound homologs from kerogen at 270 °C and the lower temperatures. If this variation were mainly due to the thermal degradation of free homologs, the 20S/(20S + 20R) ratio of $C_{29}$ steranes would have significantly increased, rather than decreased, as observed at 270 °C.

It is noteworthy that the 22S/(22S + 22R) ratio for $C_{34}$ homohopanes is higher than that of the other homohopanes for both samples YHS1 and YHS6 at 320 °C (Fig. 4a and c), consistent with the results for 27 heavy crude oils reported by Zumberge (1987).

Farrimond et al. (2003) reported the amounts and distributions of hopanoids bound to the insoluble organic matter in recent sediments from a freshwater lake (Priest Pot) and an anoxic sulphidic fjord (Framvaren) based on

**Table 3**
Molecular parameters of the pyrolysates of rock samples YHS1 and YHS6

| | Ro | OEP | Pr/$n$-$C_{17}$ | Ph/$n$-$C_{18}$ | Pr/Ph | 1 | 2 | 3 | 4 | 5 | 6 | 7 | 8 | 9 | 10 | 11 | 12 |
|---|---|---|---|---|---|---|---|---|---|---|---|---|---|---|---|---|---|
| YHS1 | | | | | | | | | | | | | | | | | |
| original | 0.42 | 0.75 | 0.61 | 1.85 | 0.32 | 0.86 | 0.563 | 0.512 | 0.489 | 0.442 | 0.430 | 0.250 | 0.282 | 0.315 | 0.130 | 0.119 | 0.154 |
| 180 °C | 0.44 | 0.72 | 2.11 | 0.23 | 0.78 | 0.62 | 0.518 | 0.495 | 0.475 | 0.502 | 0.437 | 0.245 | 0.369 | 0.364 | 0.105 | 0.084 | 0.078 |
| 210 °C | 0.47 | 0.70 | 2.04 | 0.23 | 0.76 | 0.58 | 0.512 | 0.500 | 0.482 | 0.495 | 0.455 | 0.236 | 0.373 | 0.360 | 0.102 | 0.087 | 0.078 |
| 240 °C | 0.50 | 0.70 | 2.14 | 0.21 | 0.73 | 0.50 | 0.507 | 0.496 | 0.464 | 0.517 | 0.437 | 0.201 | 0.392 | 0.343 | 0.099 | 0.080 | 0.086 |
| 270 °C | 0.53 | 0.71 | 1.95 | 0.27 | 0.75 | 0.63 | 0.512 | 0.493 | 0.457 | 0.500 | 0.414 | 0.258 | 0.367 | 0.366 | 0.109 | 0.084 | 0.074 |
| 300 °C | 0.74 | 0.79 | 1.58 | 0.39 | 0.80 | 0.65 | 0.498 | 0.507 | 0.494 | 0.514 | 0.438 | 0.294 | 0.386 | 0.338 | 0.114 | 0.083 | 0.079 |
| 320 °C | 0.86 | 0.77 | 1.22 | 0.51 | 0.79 | 0.68 | 0.535 | 0.534 | 0.518 | 0.567 | 0.524 | 0.476 | 0.407 | 0.335 | 0.114 | 0.076 | 0.068 |
| YHS6 | | | | | | | | | | | | | | | | | |
| original | 0.42 | 0.65 | 1.05 | 3.78 | 0.21 | 0.73 | 0.512 | 0.417 | 0.417 | 0.341 | 0.336 | 0.180 | 0.198 | 0.280 | 0.097 | 0.096 | 0.328 |
| 180 °C | 0.44 | 0.64 | 1.04 | 3.82 | 0.16 | 0.58 | 0.440 | 0.407 | 0.363 | 0.399 | 0.342 | 0.189 | 0.282 | 0.337 | 0.097 | 0.079 | 0.206 |
| 210 °C | 0.47 | 0.65 | 1.05 | 3.72 | 0.16 | 0.53 | 0.425 | 0.408 | 0.387 | 0.393 | 0.364 | 0.185 | 0.300 | 0.324 | 0.095 | 0.082 | 0.200 |
| 240 °C | 0.50 | 0.66 | 1.01 | 3.61 | 0.16 | 0.58 | 0.437 | 0.407 | 0.380 | 0.398 | 0.345 | 0.199 | 0.296 | 0.332 | 0.096 | 0.077 | 0.200 |
| 270 °C | 0.53 | 0.67 | 1.00 | 3.36 | 0.20 | 0.45 | 0.436 | 0.432 | 0.387 | 0.408 | 0.362 | 0.174 | 0.321 | 0.306 | 0.094 | 0.080 | 0.199 |
| 300 °C | 0.74 | 0.72 | 1.22 | 2.65 | 0.33 | 0.56 | 0.453 | 0.440 | 0.408 | 0.427 | 0.421 | 0.254 | 0.324 | 0.321 | 0.095 | 0.082 | 0.178 |
| 320 °C | 0.86 | 0.79 | 1.05 | 1.80 | 0.47 | 0.61 | 0.530 | 0.526 | 0.503 | 0.540 | 0.524 | 0.436 | 0.345 | 0.317 | 0.103 | 0.077 | 0.157 |

Ro: measured on a coal from the Jurassic coal measures in Tuha Basin, northwestern China; original: initial bitumen; 1–12: see Table 2.

catalytic hydropyrolysis analysis, and demonstrated that the bound hopanoids represent 22–30% of the total bound and solvent soluble hopanoids for sediments from Priest Pot, and 50–86% of the total for sediments from Framvaren. Those authors further demonstrated that hopanoids in a sediment from Priest Pot are almost entirely bound by strong covalent ether bonds, while the Framvaren sediment contains hopanoids that are bound by a mixture of weak disulphide and polysulphide linkages and stronger ether bonds (Farrimond et al., 2003). On this basis, we speculate that the release of the bound biomarkers could strongly influence the isomerization ratios, and the reversal of these ratios could be more likely observed during burial maturation of anoxic sulphidic sediments than freshwater lacustrine and suboxic marine shelf sediments, just as observed in the present study and by Curiale and Odermatt (1989) on phosphate/carbonate rocks from the Miocene Monterey Formation. In addition, Farrimond et al. (2003) revealed that for both the Priest Pot and Framvaren Fjord samples, the distribution patterns are $C_{31} < C_{32} > C_{33} > C_{34} < C_{35}$ for the bound homohopanes released by hydropyrolysis from kerogen, but the abundance of $C_{35}$ homohopanes is much higher for samples from Framvaren Fjord than from Priest Pot. The free homohopanes for the six samples in the present study appear somewhat similar to the bound homohopanes in distribution patterns described by Farrimond et al. (2003). Although the free homohopanes in our samples are dominantly αβ isomers, while the bound homohopanes are mainly ββ isomers (Farrimond et al., 2003), this result may imply that the release of the bound homohopanes from kerogen has strongly affected the composition of the free homohopanes in our samples.

The oil generation threshold has been suggested to be about 2800 m or 3000 m in the west Qaidam Basin in the previous studies (Hanson et al., 2001; Peng, 2005). The six samples YHS1–YHS6 are near the oil generation threshold with burial depths from 2831 to 3054 m. Farrimond et al. (1998) demonstrated that the absolute concentrations (in ppm TOC) of the free hopanes and steranes approach or exceed the maximum stage for samples around the oil generation threshold in a well in the Barents Sea. Murray et al. (1998) also demonstrated that the bound hopanes and steranes were released substantially around the oil generation threshold for Kimmeridge Clay samples (Ro% 0.45–0.55). We speculate that most bound homohopanes and steranes have been released during burial thermal maturation of the six samples YHS1 to YHS6. The variations of isomerization ratios for homohopanes and steranes with depth may result from different initial amounts and bond strengths of the bound biomarkers among these samples. Because the trend of 22S/(22S + 22R) ratios from $C_{31}$ to $C_{35}$ homohopanes within a sample in the present study is the opposite to that observed by Köster et al. (1997), it cannot be explained by steric hindrance of isomerization at C-22 of condensed type hopanoid sulphides and sulphoxides possessing the 22R stereochemistry, as suggested by Köster et al. (1997). This phenomenon observed in our study may be caused by different relative amounts of homohopanes released from kerogen with increasing the carbon number, or because homohopanes of high carbon number were released very recently compared with those of low carbon number, or both (Figs. 2 and 3).

### 3.5. Origin of low mature oils

Up to 90% of the oils found in this region have low molecular maturities (Huang et al., 1999). We analyzed 16 oil samples from the Yuejin oilfield, the largest in this area. $C_{29}$ sterane 20S/(20S + 20R) and ββ/(αα + ββ) ratios of these oils are low, generally less than 0.35. However, the amounts of saturated fractions in these oils are high (62.5–80.8%) while the total amounts of resins and asphaltenes are low (7.3–20.4%, Table 4). In addition, oils in this region have medium gravity (45.4–25.7° API) and moderate to low amounts of sulfur (0.12–0.60%, Zhu et al., 2005). Previous studies suggested that these oils were generated from source rocks at low maturity (e.g., Huang et al., 1989, 1991, 1999; Hanson et al., 2001). Based on the results of the present study and those of Farrimond et al. (2003), we present an alternative or additional mech-

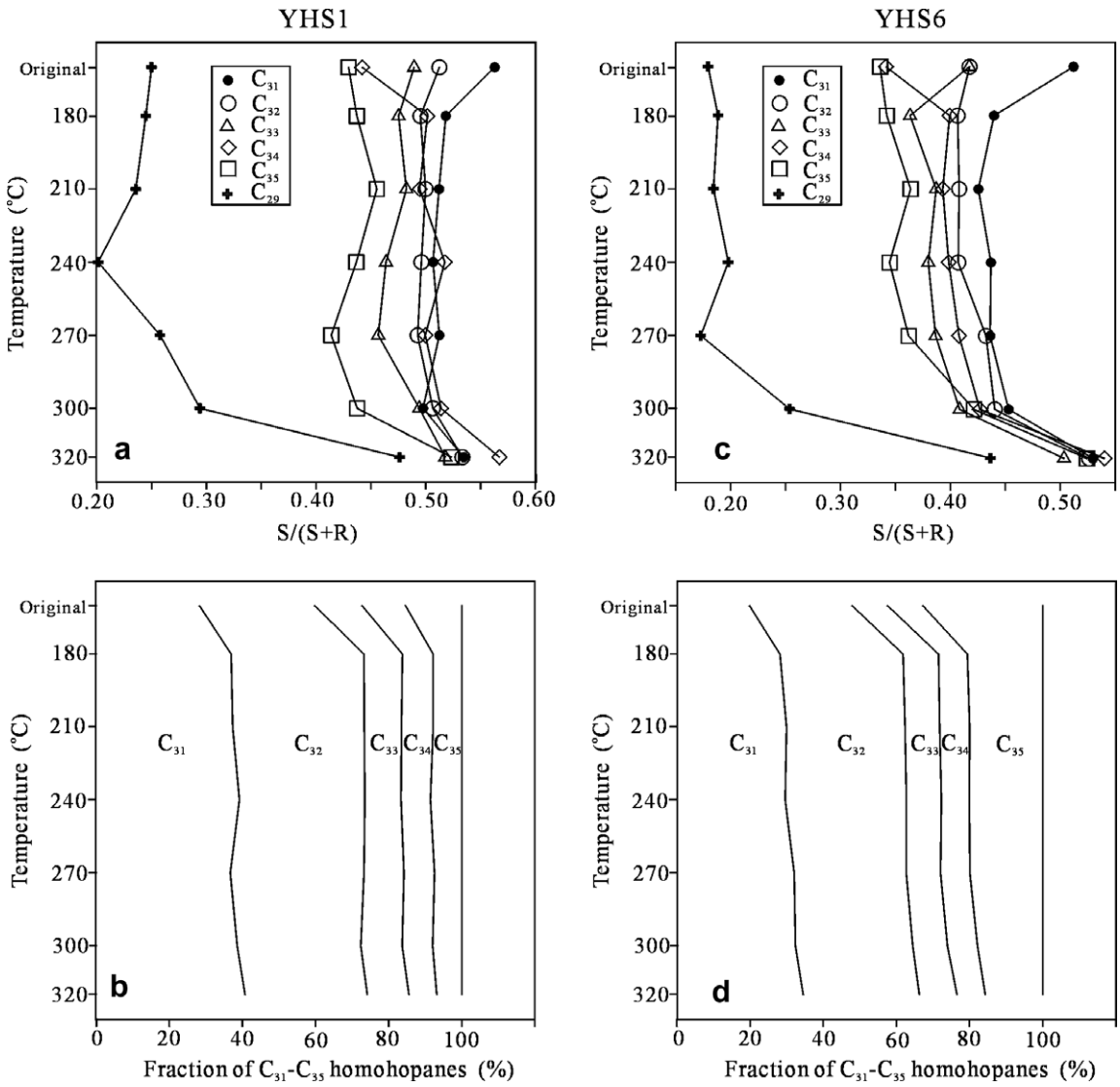


**Fig. 4.** Isomerization ratios and distribution of homohopanes and steranes in samples YHS1 and YHS6 after pyrolysis. (a and b) Sample YHS1; (c and d) sample YHS6.

anism for the origins of these low maturity oils. High amounts of bound relative to free biomarkers led to the reversal of the biomarker maturity parameters of the source rocks with burial, and resulted in relatively low biomarker maturities for the source rocks and related oils, which actually have higher thermal maturities.

Low maturity oils occur widely in China and are generally derived from anoxic, saline to brackish lacustrine source rocks containing relatively abundant carbonate minerals (e.g., Huang et al., 1999). Pang et al. (2003) suggested that immature oils in the Bamianhe oilfield of Bohai Bay Basin, eastern China, are mixtures of major amounts of mature oils with minor amounts of immature oils. Pan et al. (2007) presented a similar oil mixing mechanism for the origin of low mature oils in the Daerqi oilfield, Baiyinchagan Depression, northern China. The mechanism presented in the present study may be also applied to interpret the origins of low mature oils in the other areas of China.

## 4. Summary

The 22S/(22S + 22R) ratios for $C_{31}$–$C_{35}$ homohopanes and the 20S/(20S + 20R) ratio for $C_{29}$ steranes among six rock samples, which were deposited under saline lacustrine environments, vary significantly and irregularly with burial depth from 2831 m to 3054 m. In addition, 22S/(22S + 22R) ratios also vary substantially among $C_{31}$–$C_{35}$ homohopanes within the same sample. The ratio generally decreases from $C_{31}$ to $C_{35}$ homohopanes, a trend opposite to that reported previously by Zumberge (1987) and Köster et al. (1997). The distribution patterns of homohopanes for the six samples are unusual, e.g., $C_{31} < C_{32} > C_{33} > C_{34} < C_{35}$, or $C_{31} > C_{32} > C_{33} < C_{34} < C_{35}$, or $C_{31} < C_{32} > C_{33} < C_{34} < C_{35}$.

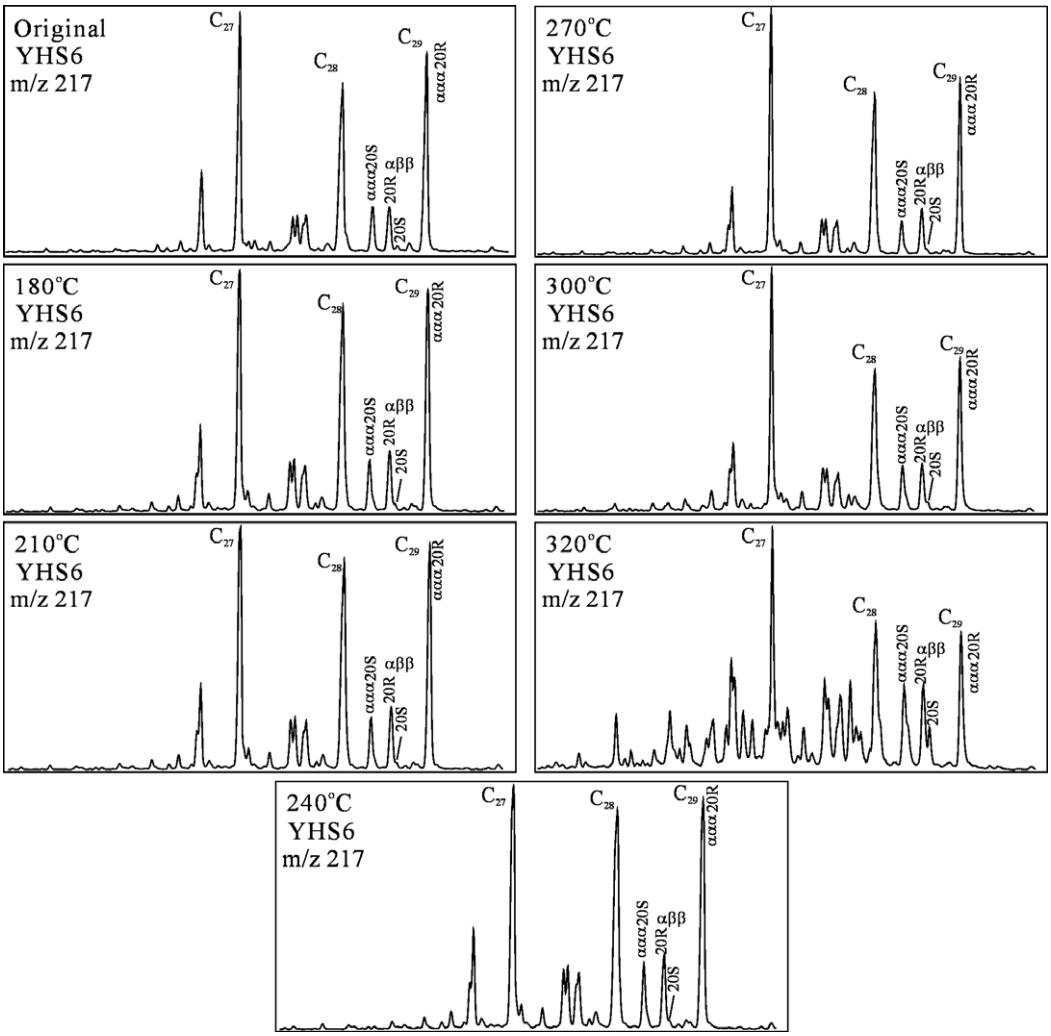


**Fig. 5.** Sterane mass chromatograms (*m/z* 217) for samples YHS6 after pyrolysis.

**Table 4**
Gross compositions and $C_{29}$ sterane isomerization ratios of oil samples from Yuejin oilfield

| Oils | Well | Depth (m) | Sat (%) | Aro (%) | Res (%) | Asp (%) | $C_{29}$ S/R | $C_{29}$ αα/ββ |
|---|---|---|---|---|---|---|---|---|
| Qx10 | Yuecan 1 | 2254.0–2447.2 | 72.2 | 13.9 | 7.6 | 6.3 | 0.32 | 0.25 |
| Qx38 | Yuecan 1 | 2254–2447.2 | 80.8 | 11.9 | 4.2 | 3.1 | 0.37 | 0.30 |
| Qx14 | Yue 355 | 1540.6–1770.3 | 62.5 | 22.0 | 10.1 | 5.4 | 0.36 | 0.32 |
| Qx15 | Yue 59 | 1613.4–1848.8 | 68.8 | 20.6 | 7.1 | 3.5 | 0.35 | 0.31 |
| Qx16 | Yue 655 | 1840.7–1981.4 | 74.3 | 12.4 | 5.7 | 7.6 | 0.31 | 0.27 |
| Qx17 | Yue 105 | 1394.4–1579.4 | 69.3 | 12.5 | 4.5 | 13.6 | 0.32 | 0.29 |
| Qx18 | Yue 2-2 | 3471.8–3528.8 | 82.1 | 6.3 | 5.3 | 6.3 | 0.33 | 0.28 |
| Qx19 | Yuexin 3-5 | 3448.4–3474.0 | 72.8 | 16.0 | 4.9 | 6.2 | 0.33 | 0.27 |
| Qx20 | Yue 19 -9 | 3552.4–3555.6 | 72.6 | 11.6 | 2.7 | 13.0 | 0.41 | 0.30 |
| Qx21 | Yue 7- 4 | 3395.4–3605.7 | 64.4 | 15.3 | 15.3 | 5.1 | 0.38 | 0.31 |
| Qx24 | Yue 7-38 | 3539.2–3626.0 | 71.5 | 12.3 | 3.8 | 12.3 | 0.42 | 0.31 |
| Qx25 | Yue 673 | 1608.2–1693.4 | 73.4 | 16.1 | 6.5 | 4.0 | 0.31 | 0.27 |
| Qx26 | Yue 573 | 1762.6–1814.0 | 74.7 | 16.4 | 6.2 | 2.7 | 0.31 | 0.28 |
| Qx35 | Yue 17 | 3368.2–3414.0 | 76.6 | 10.9 | 4.4 | 8.1 | 0.32 | 0.28 |
| Qx32 | Yue 10-10 | 3491–3622.4 | 73.0 | 12.4 | 2.2 | 12.4 | 0.40 | 0.30 |
| Qx34 | Yuedi 1 | 1366.4–1386.4 | 70.8 | 19.1 | 6.8 | 3.4 | 0.45 | 0.37 |

Sat: saturates; aro: aromatics; res: resins; asp: asphaltenes; $C_{29}$ S/R: 20S/(20S + 20R) of $C_{29}$ steranes; $C_{29}$ αα/ββ: αα/(αα + ββ) of $C_{29}$ steranes.

All of these phenomena can be mainly ascribed to the release of bound hopanes and steranes from kerogen and other macromolecules.

The 22S/(22S + 22R) ratios for $C_{31}$, $C_{32}$ and $C_{33}$ homohopanes and the 20S/(20S + 20R) ratio for $C_{29}$ steranes decreased, while the 22S/(22S + 22R) ratio for $C_{34}$ homohopanes increased for samples YHS1 and YHS6 after pyrolysis at low temperatures (180–270 °C). The distributions of homohopanes for these two samples after pyrolysis changed from their original patterns towards the pattern $C_{31} > C_{32} > C_{33} > C_{34} > C_{35}$, which is common in source rock and oil samples. In addition, the abundance of $C_{28}$ and $C_{29}$ steranes relative to $C_{27}$ steranes increased at 180–240 °C, but decreased at 270–320 °C. These results reflect the combined influences of thermal degradation and isomerization of the free biomarkers and the release of the bound biomarkers from kerogen and the other macromolecules during pyrolysis.

The results of the present study combined with the results of Farrimond et al. (2003), provide an alternative or additional mechanism for the origin of low mature oils in this region: the high amounts of bound relative to free biomarkers led to the reversal of the biomarker maturity parameters of the source rocks with burial, and resulted in relatively low biomarker maturities for the source rocks and related oils, which actually have higher thermal maturities.

## Acknowledgments

This work was jointly funded by the National Natural Science Foundation of China Grant No. 40673014 and a grant provided by the Exploration and Development Scientific Research Institute of Qinghai Oil Field Company, CNPC. We are very grateful to Drs. Maowen Li and K.E. Peters, and an anonymous reviewer for their critical comments and extensive language improvements that enormously improved our paper.

## Appendix A. Supplementary material

Supplementary data associated with this article can be found, in the online version, at doi:10.1016/j.orggeochem.2008.02.024.

*Associate Editor*—**Ken Peters**

## References

Bishop, A.N., Abbott, G.D., 1993. The interrelationship of biological marker maturity parameters and molecular yields during contact metamorphism. Geochimica et Cosmochimica Acta 57, 3661–3668.

Bishop, A.N., Love, G.D., McAulay, A.D., Snape, C.E., Farrimond, P., 1998. Release of kerogen-bound hopanoids by hydropyrolysis. Organic Geochemistry 29, 989–1001.

Curiale, J.A., Odermatt, J.R., 1989. Short-term biomarker variability in the Monterey Formation, Santa Maria Basin. Organic Geochemistry 14, 1–13.

Dzou, L.I.P., Noble, R.A., Senftle, J.T., 1995. Maturation effects on absolute biomarker concentration in a suite of coals and associated vitrinite concentrates. Organic Geochemistry 23, 681–697.

Ensminger, A., Albrecht, P., Ourisson, G., Tissot, B., 1977. Evolution of polycyclic alkanes under the effect of burial (early Toarcian shales, Paris basin). In: Campos, R., Coni, J. (Eds.), Advances in Organic Geochemistry 1975. Enadimsa, Madrid, pp. 45–52.

Ensminger, A., van Dorsselaer, A., Spyckerelle, Ch., Albrecht, P., Ourisson, G., 1974. Pentacyclic triterpenes of the hopane type as ubiquitous geochemical markers: origin and significance. In: Tissot, B., Bienner, F. (Eds.), Advances in Organic Geochemistry 1973. Editions Technip, Paris, pp. 245–260.

Farrimond, P., Bevan, J.C., Bishop, A.N., 1996. Hopanoid hydrocarbon maturation by an igneous intrusion. Organic Geochemistry 25, 149–164.

Farrimond, P., Love, G.D., Bishop, A.N., Innes, H.E., Watson, D.F., Snape, C.E., 2003. Evidence for the rapid incorporation of hopanoids into kerogen. Geochimica et Cosmochimica Acta 67, 1383–1394.

Farrimond, P., Taylor, A., Telnet, N., 1998. Biomarker maturity parameters: the role of generation and thermal degradation. Organic Geochemistry 29, 1181–1197.

Hanson, A.D., Ritts, B.D., Zinniker, D., Moldowan, J.M., Biffi, U., 2001. Upper oligocene lacustrine source rocks and petroleum systems of the northern Qaidam basin, northwest China. American Association of Petroleum Geologists Bulletin 85, 601–619.

Huang, D., Zhang, D., Li, J., Huang, X., Zhou, Z., 1989. The tertiary oil source correlation in Qaidam basin. Acta Sedimentologica Sinica 7, 1–14.

Huang, D., Li, J., Zhang, D., Huang, X., Zhou, Z., 1991. Maturation sequence of Tertiary crude oils in the Qaidam basin and its significance in petroleum resource assessment. Journal of Southeast Asian Earth Sciences 5, 359–366.

Huang, D., Zhang, D., Li, J., 1994. The origin of 4-methyl steranes and pregnanes from Tertiary strata in the Qaidam basin, China. Organic Geochemistry 22, 343–348.

Huang, D., Zhang, D., Wang, T., Wang, P., 1999. The formation mechanisms, accumulations and petroleum resource assessment of immature and low mature oils in China. Internal Research Report, CNPC, p. 669 (in Chinese).

Köster, J., Van Kaam-Peters, H.M.E., Koopmans, M.P., de Leeuw, J.W., Sinninghe Damsté, J.S., 1997. Sulphurisation of homohopanoids: effects on carbon number distribution, speciation, and 22S/22R epimer ratios. Geochimica et Cosmochimica Acta 61, 2431–2452.

Larcher, A.V., Alexander, R., Kagi, R.I., 1988. Differences in reactivities of sedimentary hopane diastereomers when heated in the presence of clays. Organic Geochemistry 13, 665–669.

Lewan, M.D., Bjorøy, M., Dolcater, D.L., 1986. Effects of thermal maturation on steroid hydrocarbons as determined by hydrous pyrolysis of Phosphoria Retort Shale. Geochimica et Cosmochimica Acta 50, 1977–1987.

Love, G.D., McAulay, A., Snape, C.E., Bishop, A.N., 1997. Effect of process variables in catalytic hydropyrolysis on the release of covalently bound aliphatic hydrocarbons from sedimentary organic matter. Energy & Fuels 11, 522–531.

Love, G.D., Snape, C.E., Carr, A.D., Houghten, R.C., 1995. Release of covalently bound alkane biomarkers in high yields from kerogen via catalytic hydropyrolysis. Organic Geochemistry 23, 981–986.

Love, G.D., Snape, C.E., Carr, A.D., Houghten, R.C., 1996. Changes in molecular biomarker and bulk carbon skeletal parameters of vitrinite concentrates as a function of rank. Energy & Fuels 10, 149–157.

Love, G.D., Snape, C.E., Fallick, A.E., 1998. Differences in the mode of incorporation and biogenicity of the principal constituents of a type I oil shale. Organic Geochemistry 28, 797–811.

Lu, S.T., Ruth, E., Kaplan, I.R., 1989. Pyrolysis of kerogens in the absence and presence of montmorillonite. I. The generation, degradation and isomerization of steranes and triterpanes at 200 and 300 °C. Organic Geochemistry 14, 491–499.

Mackenzie, A.S., Patience, R.L., Maxwell, J.R., Vandenbroucke, M., Durand, B., 1980. Molecular parameters of maturation in the Toarcian shales, Paris basin, France I. Changes in the configurations of the acyclic isoprenoid alkanes, steranes and triterpanes. Geochimica et Cosmochimica Acta 44, 1709–1721.

Mackenzie, A.S., 1984. Applications of biological markers in petroleum geochemistry. In: Brooks, J., Welte, D. (Eds.), Advance in Petroleum Geochemistry, vol. 1. Academic Press, New York, pp. 115–214.

Moldowan, J.M., Sundararaman, P., Salvatori, T., Alajbeg, A., Gjukic, B., Lee, C.Y., Demaison, G.J., 1992. Source correlation and maturity assessment of select oils and rocks from the Central Adriatic Basin (Italy and Yugoslavia). In: Moldowan, J.M., Albrecht, P., Philp, R.P. (Eds.), Biological Markers in Sediments and Petroleum. Prentice-Hall, Englewood Cliffs, NJ, pp. 370–401.

Monthioux, M., Landais, P., Durand, B., 1986. Comparison between extracts from natural and artificial maturation series of Mahakam Delta coals. Organic Geochemistry 10, 299–311.

Monthioux, M., Landais, P., Monin, J.-C., 1985. Comparison between natural and artificial maturation series of humic coals from the Mahakam Delta, Indonesia. Organic Geochemistry 8, 275–292.

Murray, I.P., Love, G.D., Snape, C.E., Bailey, N.J.L., 1998. Comparison of covalently bound aliphatic biomarkers released via hydropyrolysis with their solvent-extractable counterparts for a suite of Kimmeridge Clays. Organic Geochemistry 29, 1487–1505.

Ourisson, G., Albrecht, P., Rohmer, M., 1979. The hopanoids, paleochemistry and biochemistry of a group of natural products. Pure and Applied Chemistry 51, 709–729.

Ourisson, G., Albrecht, P., Rohmer, M., 1984. The microbial origin of fossil fuels. Scientific American 251, 34–41.

Pan, C., Tan, Y., Feng, J., Jin, G., Zhang, Y., Sheng, G., Fu, J., 2007. Mixing and biodegradation of hydrocarbons in the Daerqi oilfield, Baiyinchagan Depression, northern China. Organic Geochemistry 38, 1479–1500.

Pan, C., Yu, L., Liu, J., Fu, J., 2006. Chemical and carbon isotopic fractionations of gaseous hydrocarbons during abiogenic oxidation. Earth and Planetary Science Letters 246, 70–89.

Pang, X., Li, M., Li, S., Jin, Z., 2003. Petroleum systems in the Bohai Bay Basin. Part 2. Geochemical evidence for significant contribution of mature source rocks to "immature oils" in the Bamianhe field. Organic Geochemistry 34, 931–950.

Peng, D., 2005. Hydrocarbon generation from Tertiary saline lacustrine source rocks in the Western Qaidam Basin, northwest China. Ph.D. Dissertation, Guangzhou Institute of Geochemistry, Chinese Academy of Sciences.

Peters, K.E., Moldowan, J.M., Sundararaman, P., 1990. Effects of hydrous pyrolysis on biomarker thermal maturity parameters: Monterey phosphatic and siliceous members. Organic Geochemistry 15, 249–265.

Peters, K.E., Moldowan, J.M., 1991. Effects of source, thermal maturity, and biodegradation on the distribution and isomerization of homohopanes in petroleum. Organic Geochemistry 17, 47–61.

Peters, K.E., Moldowan, J.M., 1993. The Biomarker Guide: Interpreting Molecular Fossils in Petroleum and Ancient Sediments. Prentice-Hall, Englewood Cliffs, NJ.

Peters, K.E., Walters, C.C., Moldowan, J.M., 2005. The Biomarker Guide. Biomarkers and Isotopes in Petroleum Exploration and Earth History, vol. 2. Cambridge University Press, UK.

Requejo, A.G., 1994. Maturation of petroleum source rocks. II. Quantitative changes in extractable hydrocarbon content and composition associated with hydrocarbon generation. Organic Geochemistry 13, 91–105.

Seifert, W.K., Moldowan, J.M., 1980. The effect of thermal stress on source-rock quality as measured by hopane stereochemistry. In: Douglas, A.G., Maxwell, J.R. (Eds.), Advances in Organic Geochemistry 1979. Pergamon Press, Oxford, pp. 229–237.

Seifert, W.K., Moldowan, J.M., 1986. Use of biological markers in petroleum exploration. In: Johns, B.R. (Ed.), Biological Markers in the Sedimentary Record. Elsevier, Oxford, pp. 261–290.

Sinninghe Damsté, J.S., van Duin, A.C., Hollander, D., Kohnen, M.E.L., de Leeuw, J.W., 1995. Early diagenesis of bacteriohopanepolyols derivates: formation of fossil homohopanoids. Geochimica et Cosmochimica Acta 59, 5141–5157.

Strachan, M.G., Alexander, R., Subroto, E.A., Kagi, R.I., 1989. Constraints upon the use of 24-ethylcholestane diastereomer ratios as indicators of the maturity of petroleum. Organic Geochemistry 14, 423–432.

Van Duin, A.C., Sinninghe Damsté, J.S., Koopmans, M.P., van de Graaf, B., de Leeuw, J.W., 1997. A kinetic calculation method of homohopanoid maturation: applications in the reconstruction of burial histories of sedimentary basins. Geochimica et Cosmochimica Acta 61, 2409–2429.

Zhu, Y., Weng, H., Su, A., Liang, D., Peng, D., 2005. Geochemical characteristics of Tertiary saline lacustrine oils in the Western Qaidam Basin, northwest China. Applied Geochemistry 20, 1875–1889.

Zumberge, J.E., 1987. Terpenoid biomarker distributions in low maturity crude oils. Organic Geochemistry 11, 479–496.